Canadian Journal of Pure and Applied Sciences
Vol. 13, No. 1, pp. 4733-4746, Feb 2019
Online ISSN: 1920-3853; Print ISSN: 1715-9997
Available online at www.cjpas.net

NET-SAND ESTIMATION USING SEISMIC ANISOTROPY MODELING IN THE CENTRAL NIGER DELTA

*God'swill I. Alaminiokuma and Jonathan I. Omigie
Department of Earth Sciences
Federal University of Petroleum Resources Effurun
PMB. 1221, Effurun, Warri, Nigeria

ABSTRACT

Net-sand was estimated using seismic anisotropy modelling in the Central Niger Delta. Gamma ray Logs, Pre SDM and PSDM seismic data from Kolo Creek Field were analyzed. A correlation of Hockey stick effects and seismic eta values which vary laterally with geologic surfaces confirmed the presence of anisotropy within the Field. Seismic eta cubes were generated along 11.5MFS, 12.1SB, 12.8MFS, 13.1SB, 15.0MFS, 15.5SB, 15.9MFS and 16.7SB geologic surfaces each having interval thickness lying between 150 to 250 m. Volume of shale, V_s calculated from Gamma ray logs was cross-plotted with seismic eta, η values derived from seismic anisotropy processing. Results obtained showed that a linear relationship exist between eta, η and volume of shale, V_{sh}. This was then used to estimate the interval net-sand of the region for which eta cube has been obtained. The results obtained were consistent with predictions made by other researchers using different methods. This study is useful for accurate estimation of the total volume of sand of a reservoir and is also essential for estimating the amount of hydrocarbon in place and also allows for proper additional placement of wells to optimally drain a reservoir.

Keywords: Niger Delta, Kolo creek field net-sand, seismic anisotropy, eta cube, shale volume.

INTRODUCTION

The Niger Delta is made up of heterogeneous formations with sands and shales interbedded in alternating sequence (Short and Stauble, 1967). The aggregate of these sand and shale interbeds makes up the *Gross Sand.* The gross sand is made up of a top and a base usually mapped using seismic data and or well data. Distinct sand units can be mapped within the gross sand but the low resolution of seismic data within these small units makes this difficult. It is more realistic to map the *Net-Sand* thickness in the gross sand. Knowledge of the net-sand thickness over the entire lateral extent of the gross sand allows for accurate prediction of the total volume of sand of a reservoir and is essential for estimating the amount of hydrocarbon in place and also allows for proper additional placement of wells to optimally drain a reservoir.

Various researchers have employed different methods to estimate the net-sand thickness from seismic and well data (Brown *et al.,* 1984; Burge and Neff, 1998; Connolly *et al.*, 2002; Connolly, 2005; Kishore, *et al*., 2006; Chunduru and Nordstrom, 2008; Simm, 2009). Net-sand estimation, by these researches was based on the assumption that the subsurface behaves seismically isotropic, that is, the intrinsic elastic properties of the medium measured at the same location do not change with direction. Seismic anisotropy which considers the directional dependence of rock properties within a particular location is important for seismic imaging, seismic interpretation, and reservoir characterization (Li, 2004). Significantly, seismic anisotropy has been very useful in reservoir sand estimation (Ouadfeul, 2015; Li, 2004; Alkhalifah and Rampton, 2001; Okorie *et al*., 2016).

This research predicts interval net-sand regimes over a broad range of gross sand thickness using seismically-derived anisotropy eta, η tied to volume of shale, V_{sh} generated from Gamma ray log and net-to-gross (N/G) in order to identify geologic sources and the effects of the lateral and vertical seismic anisotropy observed in the Central Niger Delta.

LOCATION AND GEOLOGY OF THE STUDY AREA

The area under study is the Kolo Creek (Fig. 1), an onshore Field located within OMLs 35 and 36 in the Central Swamp depobelt of the Niger Delta. The Field has an aerial extent of about 5x10 km. The main reservoir is the E2.0 which is oil bearing with depth ranging from 3580 to 3670 meters and is about 50 - 60 meters thick.

*Corresponding author e-mail: alaminiokuma.godswill@fupre.edu.ng

The sedimentary sequence is mainly deltaic depositional sub-environments (Oboh, 1995). The lithofacies identified are rich in palynodebris, wood fragments, black debris and amorphous organic matter. The palynomorph assemblage has been used to date the reservoir to the early part of the middle Miocene (14 to 15 Ma before present), which has been identified to be deposited in parasequenece of shallow marine and deltaic plain deposits (Oboh, 1995). The Field is characterized by numerous predominantly E–W trending growth faults with reservoirs that are of the Middle Miocene and of the Agbada Formation (Oboh, 1993).

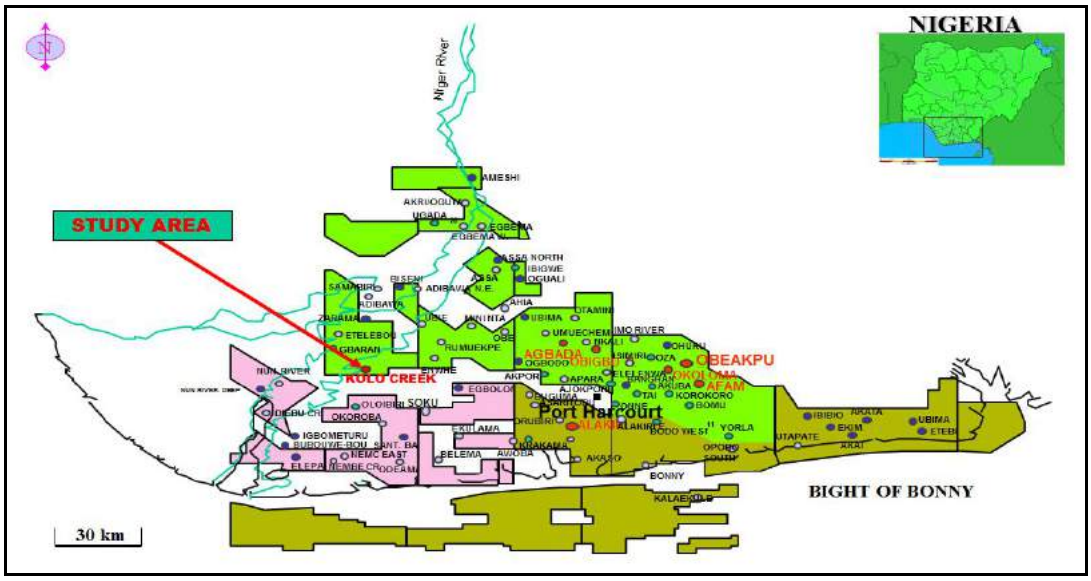

Fig. 1. Location map showing the Kolo Creek field in the Central Niger Delta.

MATERIALS AND METHODS

Methodology

Work Flow: Figure 2 is a chart of the net-sand estimation using well log and seismic data.

Data

Figure 3 shows a traverse of Prestack Depth Migrated seismic volume in Kolo Creek Field displayed at the background. Also available for this Field is the long cable PSDM shot gathers. The data were analyzed using the following software: 123DI^{TM}, Savior^{TM}, and Rokdoc^{TM}.

Data Analysis

The gamma ray logs were digitized to identify and map the various lithologic units (shale intervals). Reservoir tops and bases were mapped to identify units and tie the well tops to seismic reflectivity. The seismic data were analyzed to determine the delta, δ required for well-to-seismic tie and for effective time-to-depth conversion. A delta, δ of 0.2 instead of 0.0 was used in processing the seismic data.

The core data obtained by Thomsen (1986) and the Chart by Li (2004) were carefully studied in order to deduce and adapt the established relationship between epsilon, ε seismic velocity, V and shale volume, V_{sh}.

Generation of Volume of Shale, V_{sh}

To determine the volume of shale, the gamma ray index I_{GR} was calculated applying the Equation (Schlumberger, 1996) in ***Rokdoc^{TM}*** software:

$$I_{GR} = \frac{(GR_{\log} - GR_{\min})}{(GR_{\max} - GR_{\min})} \quad (1)$$

Where I_{GR} = gamma ray index; GR_{log} = Gamma ray reading of the Formation; GR_{min} = minimum Gamma ray reading (clean sand); GR_{max} = maximum Gamma ray reading (shale baseline)

Generation of Eta Cube

Figure 3 shows the mapped geologic surfaces, the seismic eta cube and gamma ray log of the well Kolo Creek-039ST1. It can be observed that real geologic surfaces with ages were available within the interval of the seismic eta cube. The seismic eta cube is made up of eight geologic surfaces which include: 11.5MFS, 12.1SB, 12.8MFS, 13.1SB, 15.0MFS, 15.5SB, 15.9MFS and 16.7SB with the successive geologic surfaces having interval thickness lying between 150 to 250 m. This implies that the geologic surfaces are more finely defined. The bands of the seismic eta cube were observed to be laterally flat and having a constant eta, η value along the vertical axis within an eta band. However, there are lateral variations of seismic eta value within each eta band which can be inverted to volume of shale variation.

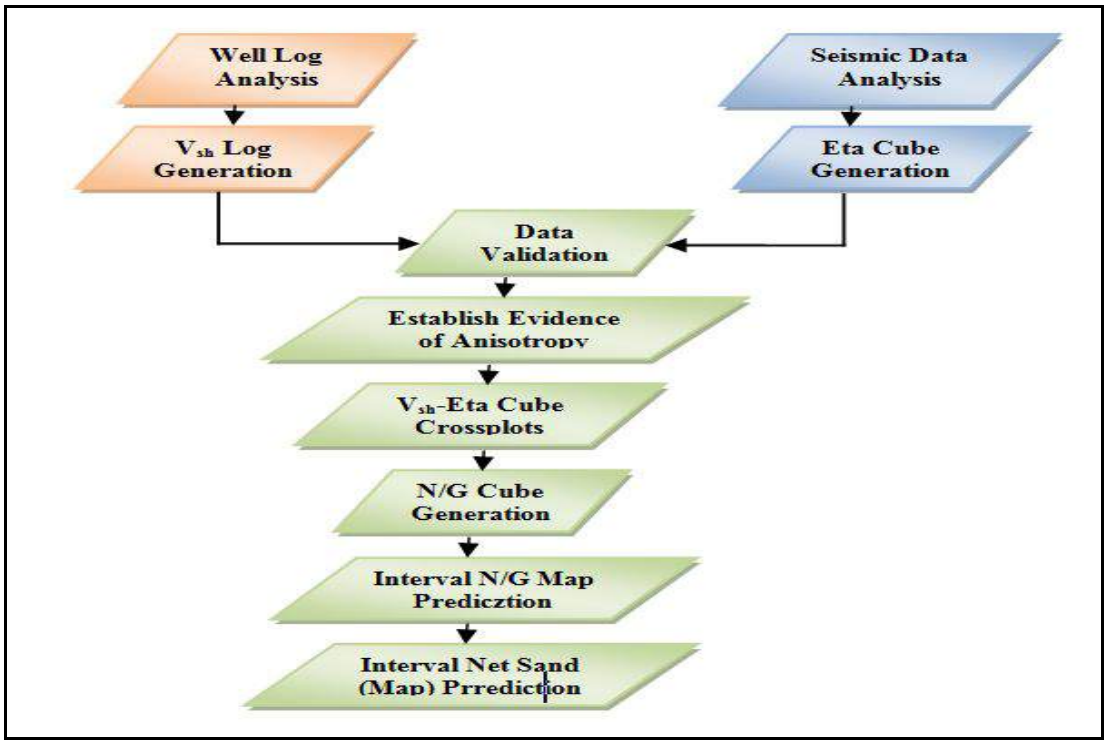

Fig. 2. Chart showing the Sequence of Data analysis.

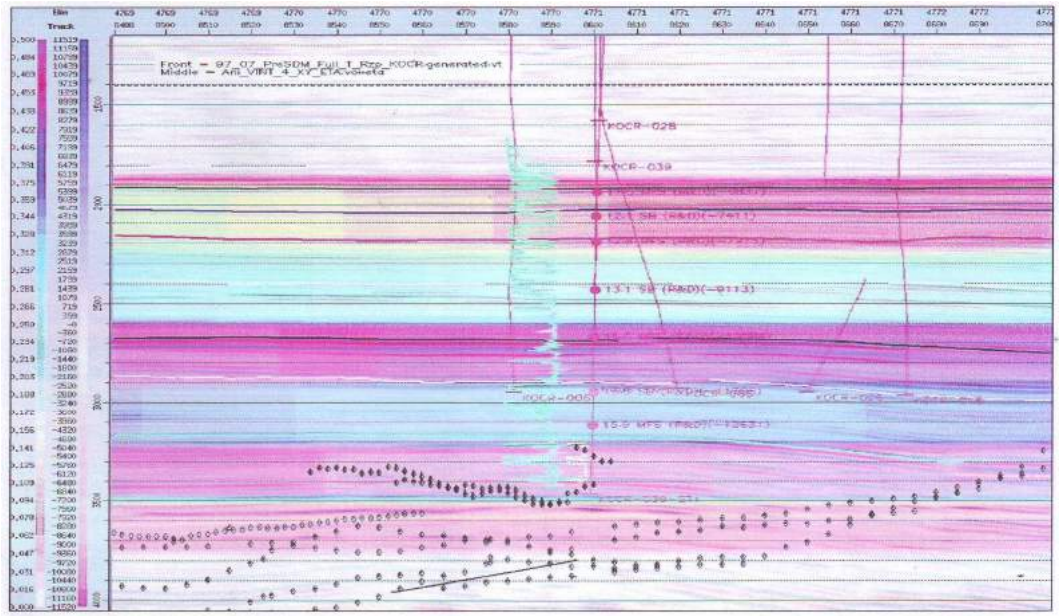

Fig. 3. Traverse of the Kolo Creek Field Seismic Eta Cube of with PreStack Depth Migrated Seismic Volume Displayed at the Background.

Data Validation

The GR logs and the generated shale log were validated to check the consistency of these logs with geologic intervals. Similarly, the eta cube was validated by checking how the variations in the values of seismic eta, η correspond to the variation in the nature of hockey sticks observed. Geologic markers from well logs were also used to validate the interpreted seismic horizons.

Evidence of Anisotropy in Kolo Creek Field

The presence of anisotropy in the region was confirmed by analysing the PSDM gathers to identify hockey stick effects (Fig. 4). It is observed that the hockey stick effects

are present and more severe at about 3.2s as shown in the black loop in Figures 5(a to c). This is an indication that the main source of hockey stick effects is located at shallower depths than 3.2s. With the aid of gamma ray log, thick shale formation was identified above the depth (3.2s) where the hockey stick effects are very severe. This shale formation lies between 13.1SB and 15.5SB and this is believed to be main source of anisotropy in this Field (Johnston and Christensen, 1995).

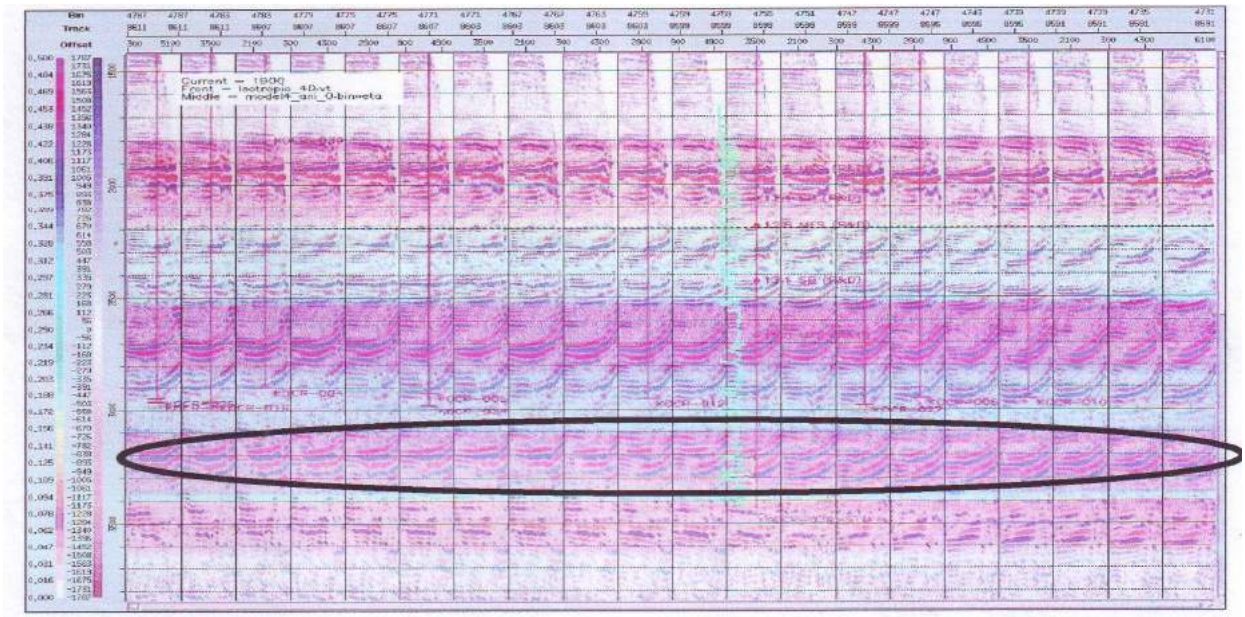

Fig. 4. Traverse of the Kolo Creek PSDM Shot gathers showing observed Hockey Stick Effects.

Correlation reveals that a lateral variation exists between hockey sticks and seismic eta values extracted along geologic surfaces in this Field. Various traverse lines in different directions crossing different eta values were considered to observe the change in hockey sticks from one eta value to another.

Figures 5a, 5b and 5c show the different types of hockey sticks for various values of seismic eta. Areas of high values of eta, η are observed to correspond to severe hockey stick effects.

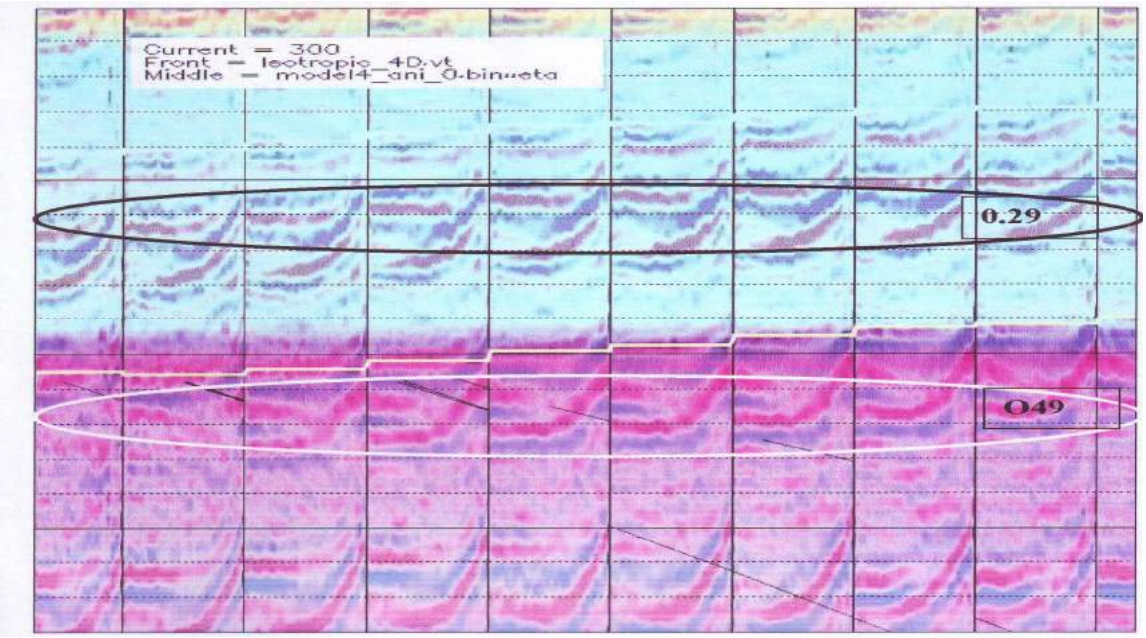

Fig. 5a. Hockey Sticks effects corresponding to Seismic Eta values of 0.49 and 0.29.

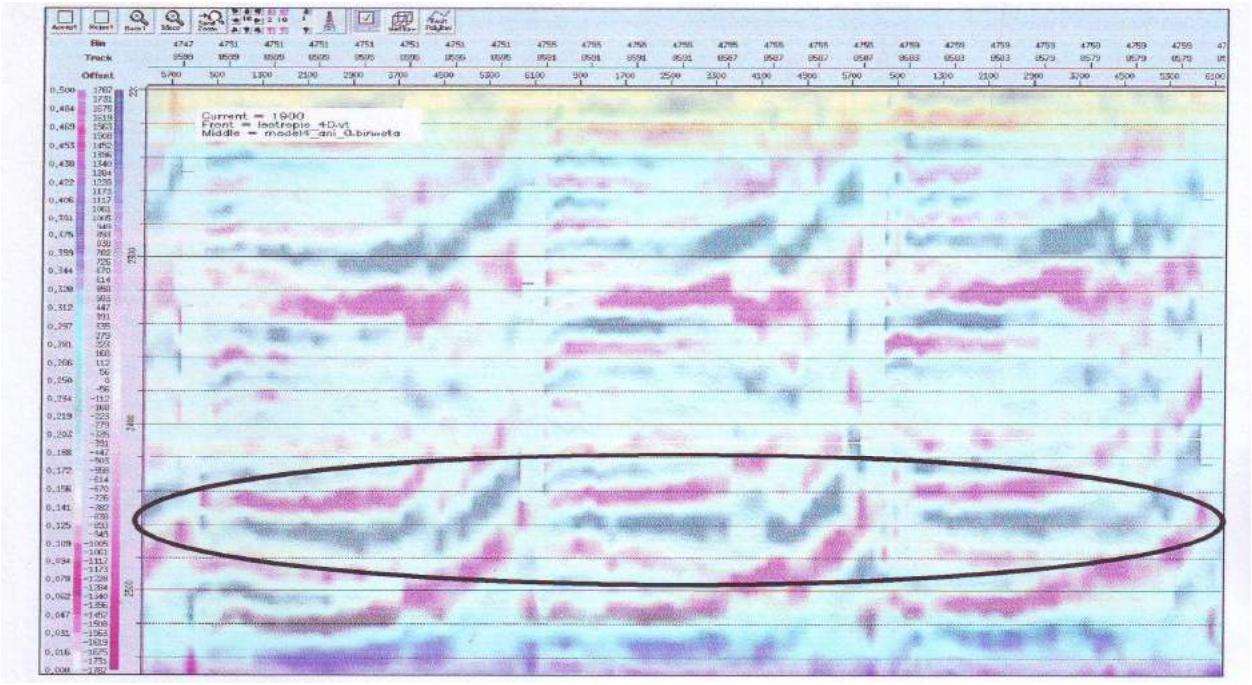

Fig. 5b. Hockey Sticks effects corresponding to Seismic Eta values of 0.196.

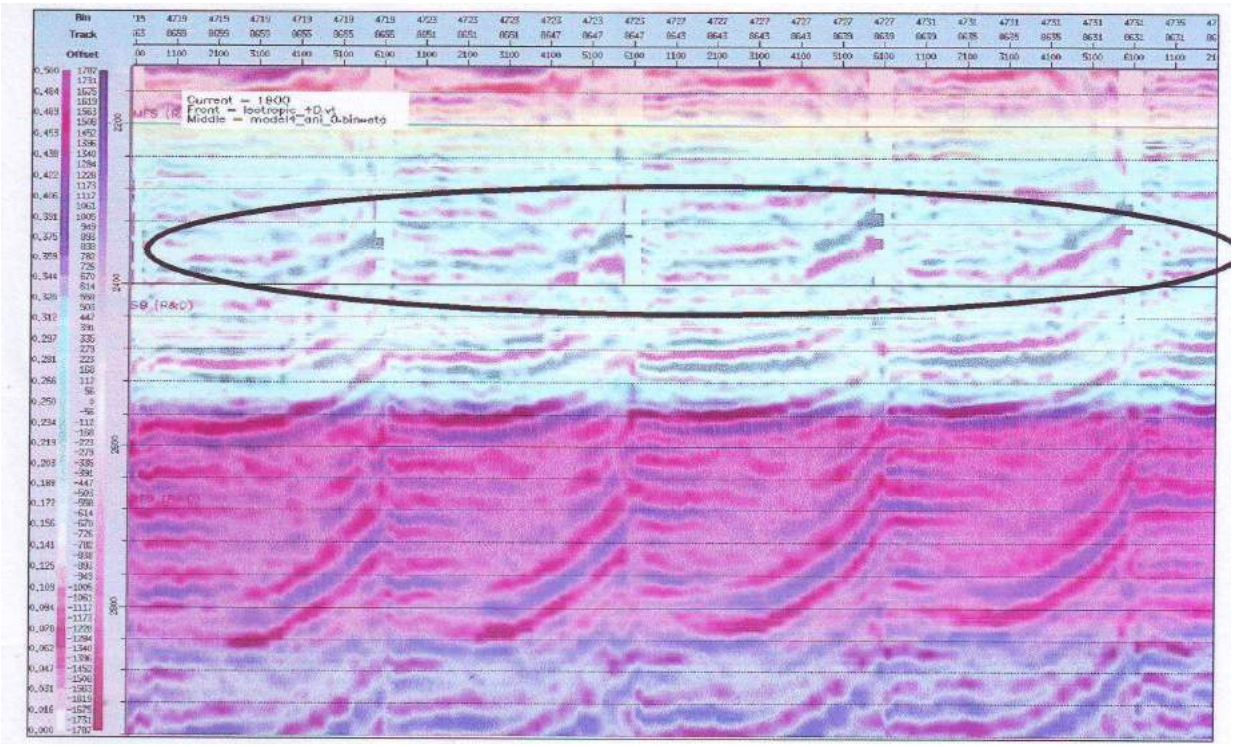

Fig. 5c. Hockey Sticks effects corresponding to Seismic Eta values of 0.201.

Crossplots of Eta Cube - Shale Volumes, V_{sh}

Crossplots of Eta cube-Volume of shale were generated to establish a relationship between Eta cube and volume of shale. Data points were obtained by sampling the Eta cube along the well paths of some selected wells and then sampling the average volume of shale in the interval of Eta cube samples.

Net-to-Gross Sand Maps

Net-to-Gross cubes, net-to-gross and net sand maps were generated by using the trends obtained from the crossplots as inputs into *Savior*^{TM} *Software* (Volume Calculator), *Attribute Extraction (lama*) and *Event Calculator*. Gross thicknesses were also obtained using the *Attribute Extraction*.

RESULTS AND DISCUSSION

Eta Maps

The lateral variation of Eta, η was observed and Eta maps were produced for the two mapped horizons. The results are shown in Figures 6. Here, a general trend of seismic Eta increasing southwards from the major fault can be observed.

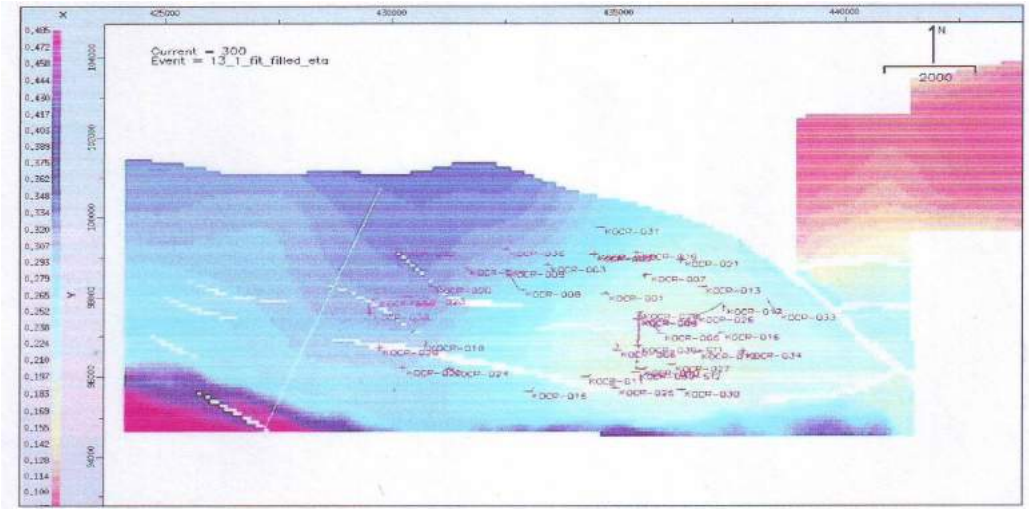

Fig. 6. Typical Map showing Seismic Eta Values Extracted along the 13.1SB Horizon.

Volume of Shale, V_{sh} - Seismic Eta, η Crossplots

A relationship between Volume of Shale, V_{sh} and Seismic Eta, η was established by extracting Eta values along the well paths (KOCR-002, KOCR-003, KOCR-006, KOCR-011, KOCR-012, KOCR-018, KOCR-020, KOCR-030, KOCR-035, KOCR-039ST1) sampled at an interval of 40ft. Gamma Ray logs from these wells were exported to *Rockdoc*^{TM} to generate the volume of shale logs and then 'blocked' in order to obtain the average volume of shale within the sampling interval (Fig. 7).

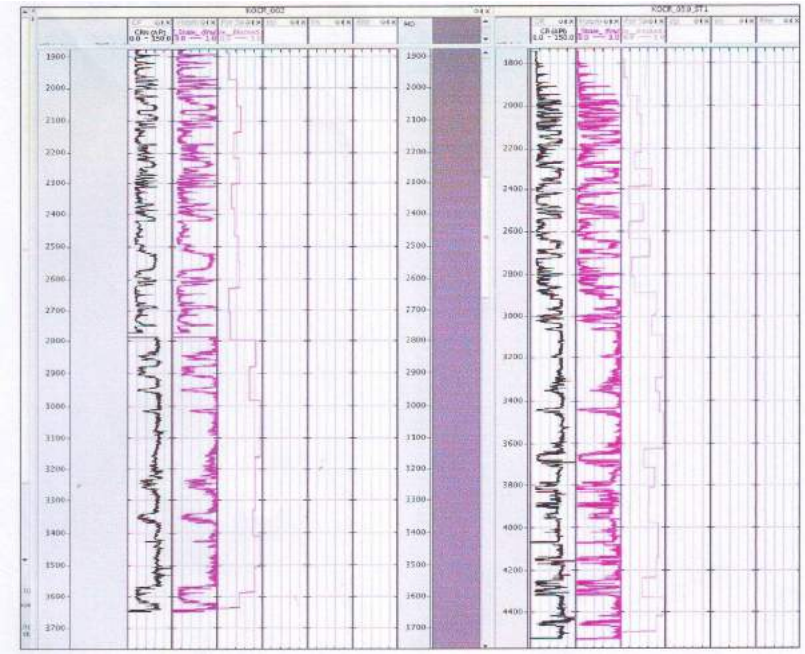

Fig. 7. Log Panel from *Rockdoc* showing GR, calculated blocked V_{sh} Logs for KOCR-002 and KOCR-039ST1.

The values of eta, η sampled in this process were then compared with the values of volume of shale, V_{sh} at the same interval. A crossplot of Volume of shale, V_{sh} versus Seismic *eta*, η was produced and the relationship shown in Figure 8. Three linear trends: Maximum V_{sh} (red), most like V_{sh} (black) and minimum V_{sh} (yellow) were produced to check the uncertainty in the data points. Equations (2), (3) and (4) respectively represent the linear functions of these plots.

$$V_{sh(\max)} = 0.921\eta + 0.517 \quad (2)$$

$$V_{sh(ml)} = 1.1255\eta + 0.893 \quad (3)$$

$$V_{sh(\min)} = 1.41\eta \quad (4)$$

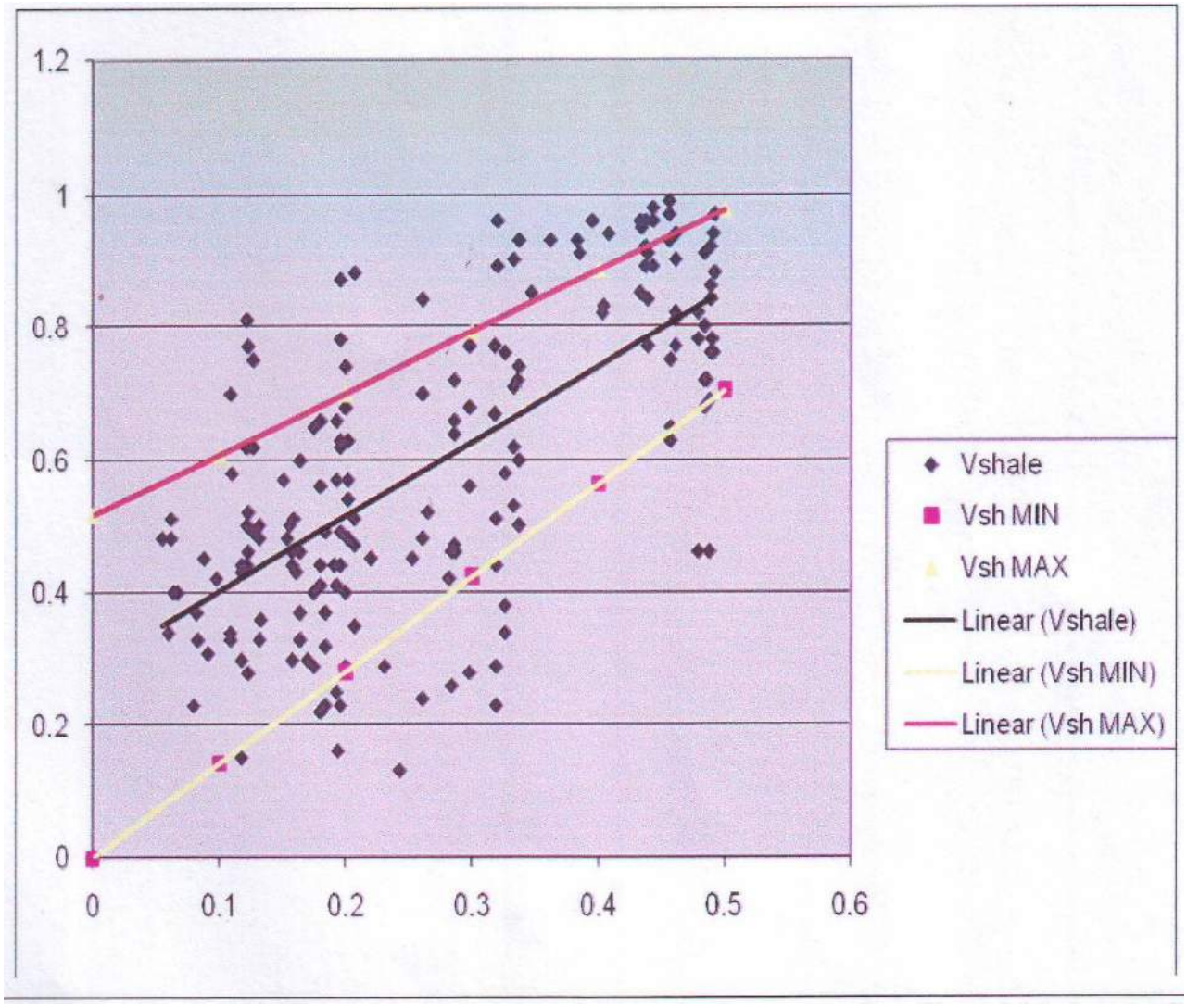

Fig. 8. Volume of shale, V_{sh}-Eta, η Crossplot.

Net-to-Gross Cubes

Equations (2), (3) and (4) which have direct relationship with *eta*, η were employed to construct net-to-gross cubes, interval net maps and net sand maps following the sequence in Figure 2. Maximum net-to-gross cube was constructed by Equation (2) for which *eta* has direct relationship with minimum volume of shale. The most likely net-to-gross cubes were constructed by Equation (3) for which *eta* has direct relationship with the most likely volume of shale while minimum net-to-gross cubes was constructed using Equation (4) for which *eta* has direct relationship with maximum volume of shale. These are shown in Figures 9a, 9b, and 9c, respectively.

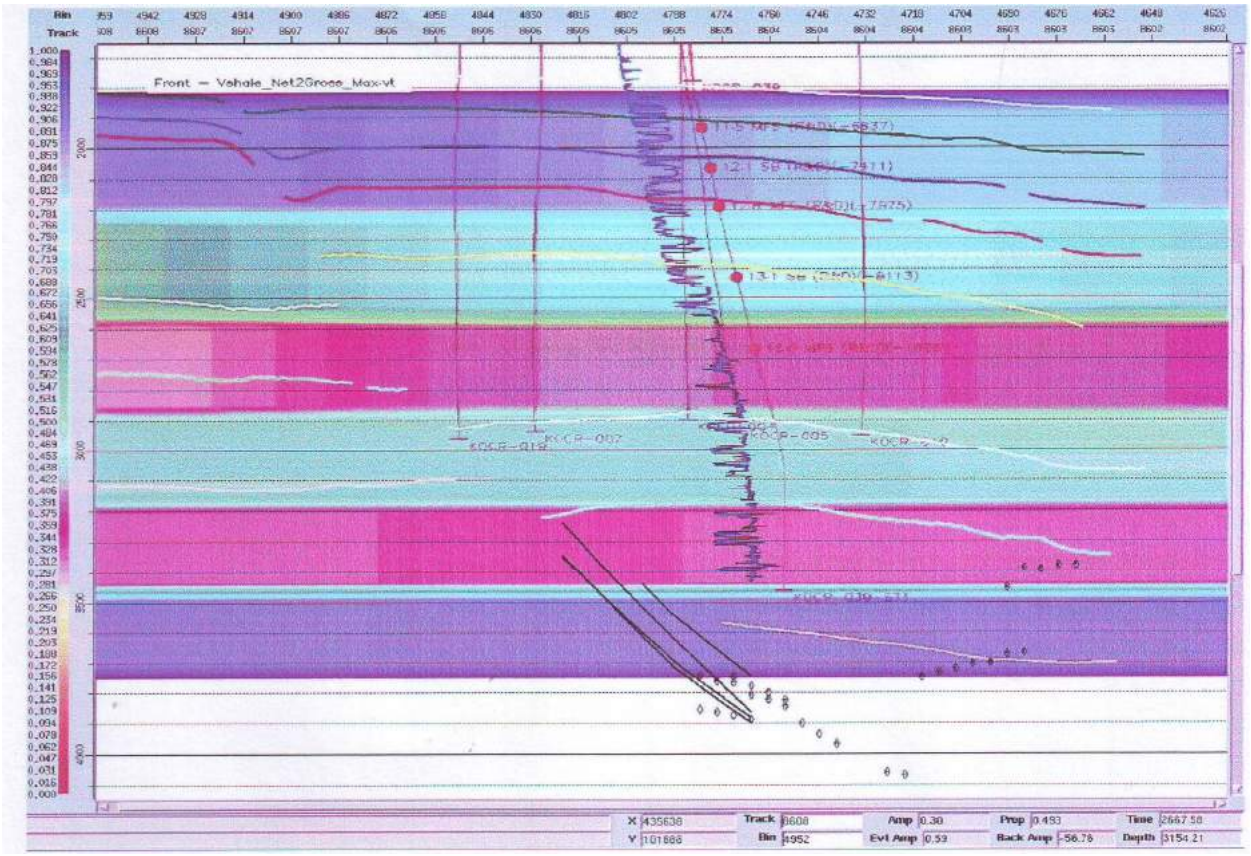

Fig. 9a. Predicted Maximum Net-to-Gross Cube.

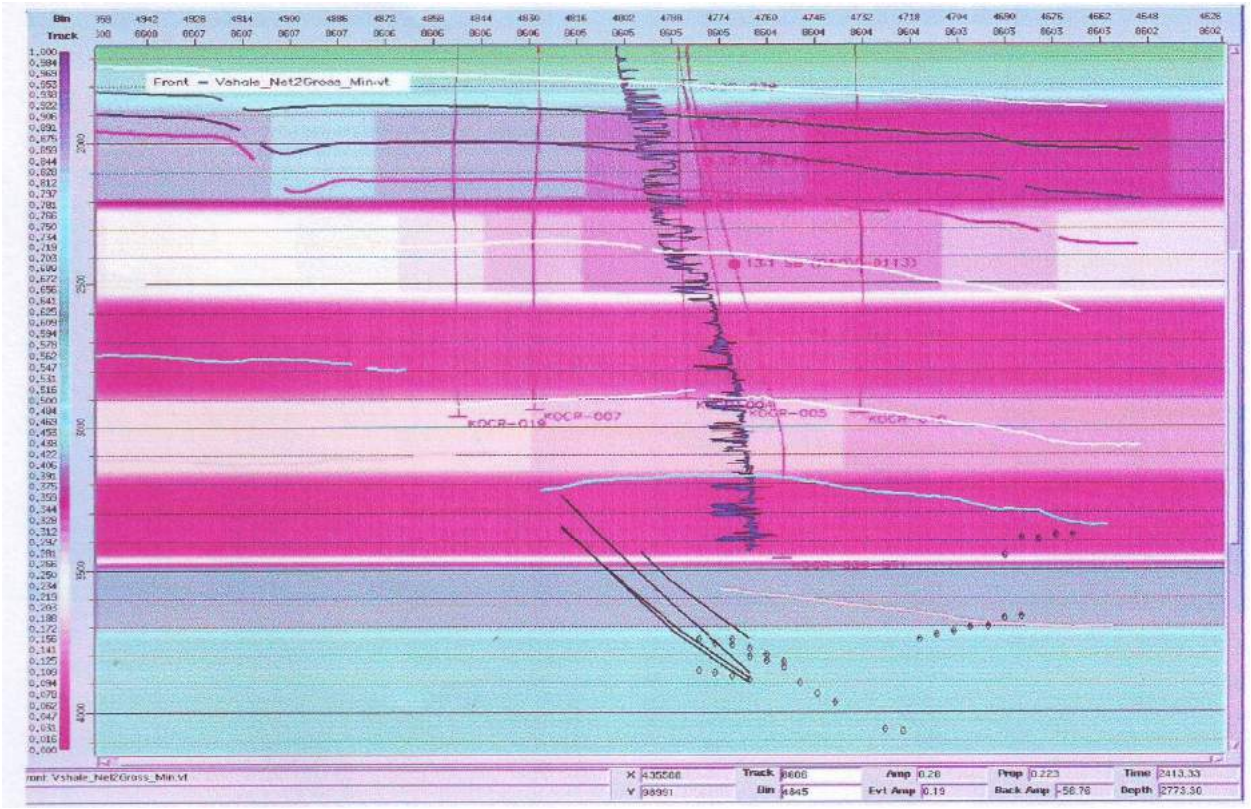

Fig. 9b. Predicted Minimum Net-to-Gross Cube.

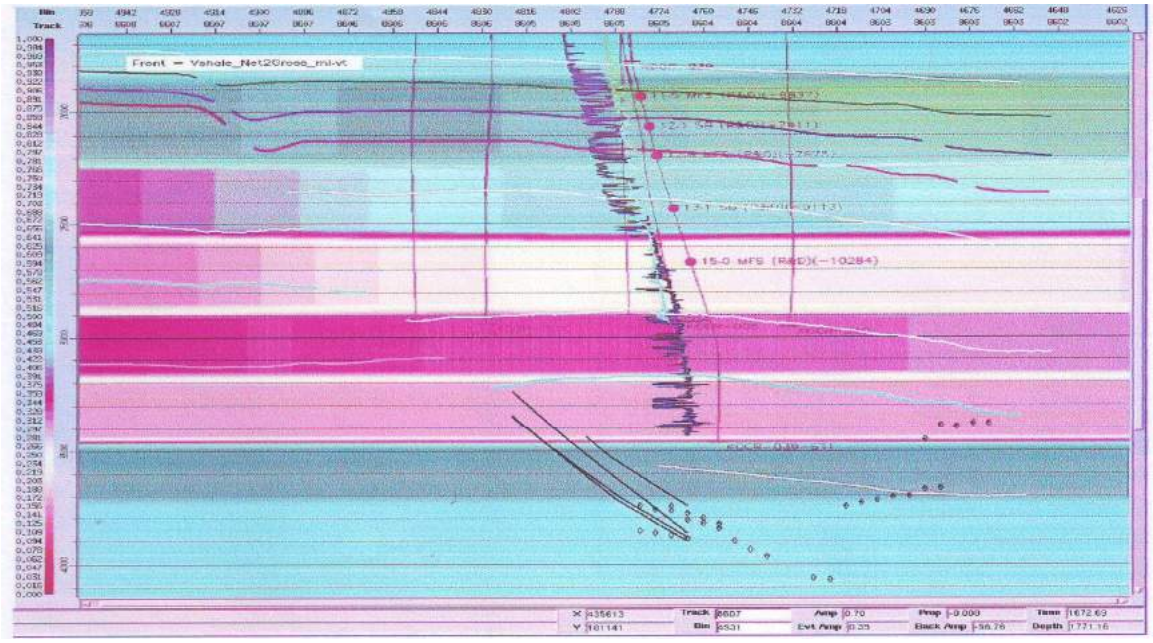

Fig. 9c. Predicted Most-likely Net-to-Gross Cube.

The gamma ray logs of the sampled wells were displayed on the constructed net-to-gross cube to check the accuracy of the predictions around the well control. Further quality-checking of the predictions was conducted by using gamma ray logs from other wells in the Field. This provides a measure of how accurate the predictions are away from the well.

Net-to-Gross Maps

Figure 10 is a net-to-gross map for the interval 12.1SB to 15.0MFS showing well paths and traverse lines. The traverse lines of the predicted most-likely net-to-gross are shown in Figure 11. The wells displayed in black have the logs used in the sampling process. The wells displayed in red were not included in the sampling process. It can be observed that regions of high and low net-to-gross as predicted by the net-to-gross cube correspond to regions of low and high volume of shale measurements respectively for both sampled and unsampled wells. These findings increase confidence in the predicted net-to-gross values away from the well controls.

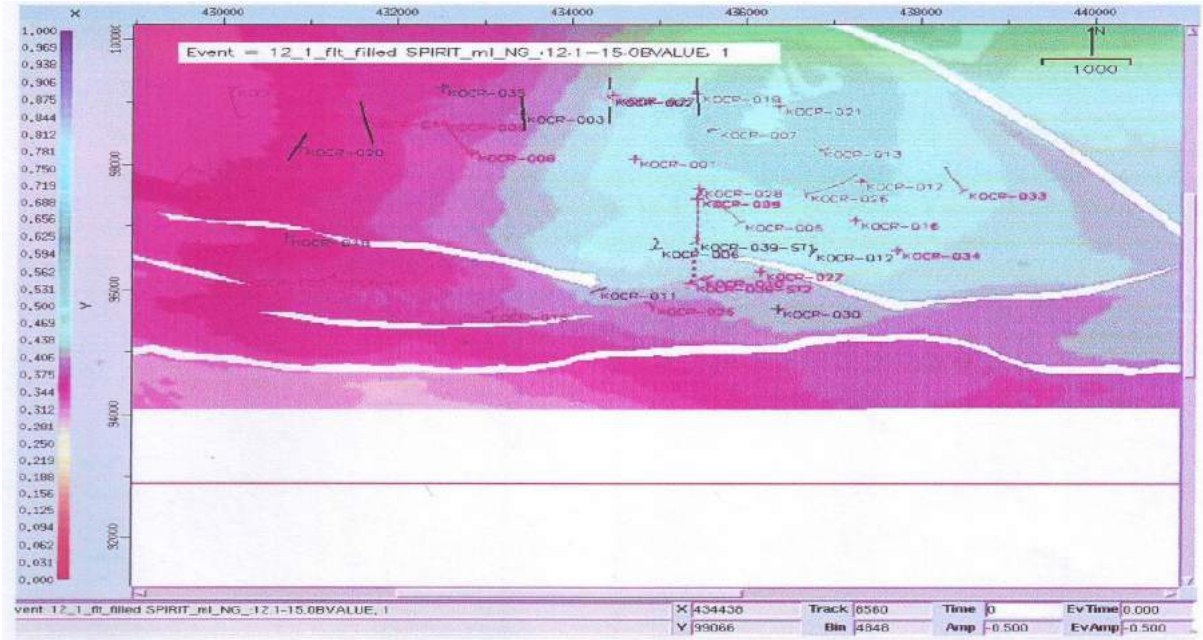

Fig. 10. Map of Net-to-Gross from 12.1SB to 15.0MFS showing Well Paths and Traverse Lines.

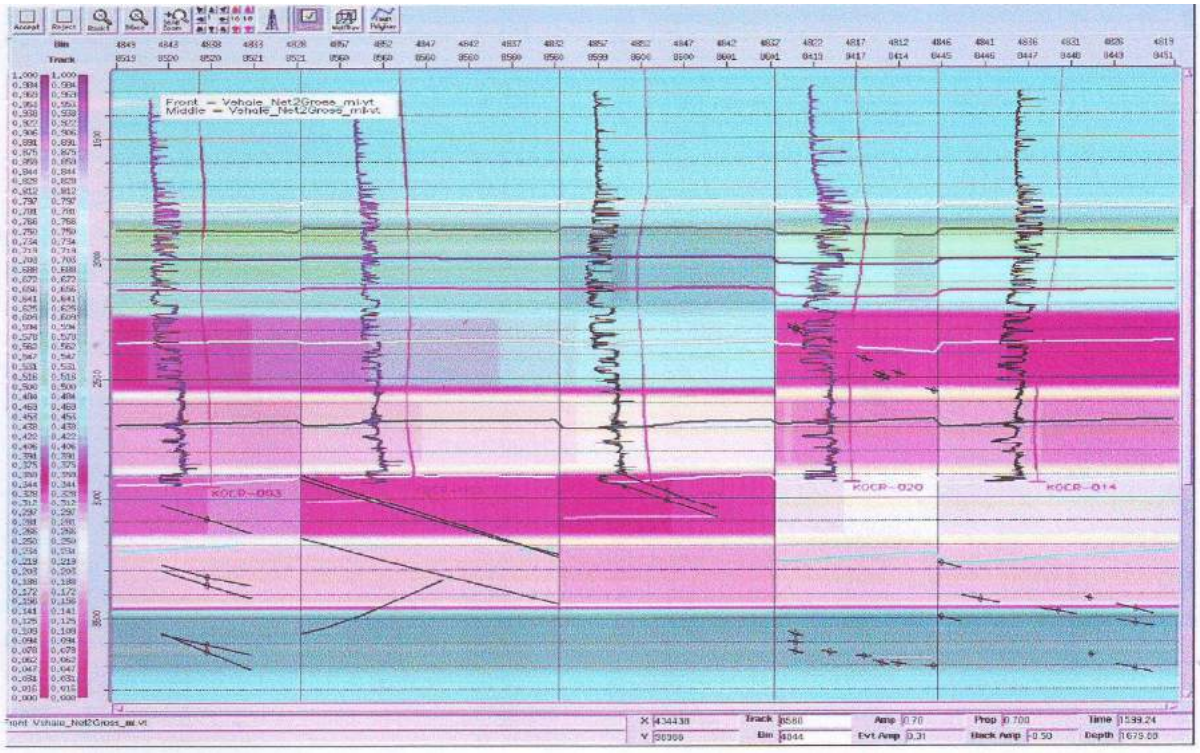

Fig. 11. Well Traverse of Predicted most-likely Net-to-Gross Volumes.

From the net-to-gross volumes, net-to-gross maps were produced for various intervals. Figures 12a, 12b and 12c are map views showing the interval net-to-gross for the maximum, most-likely and minimum net-to-gross predictions respectively. The interval used is the 12.8MFS to 13.1SB.

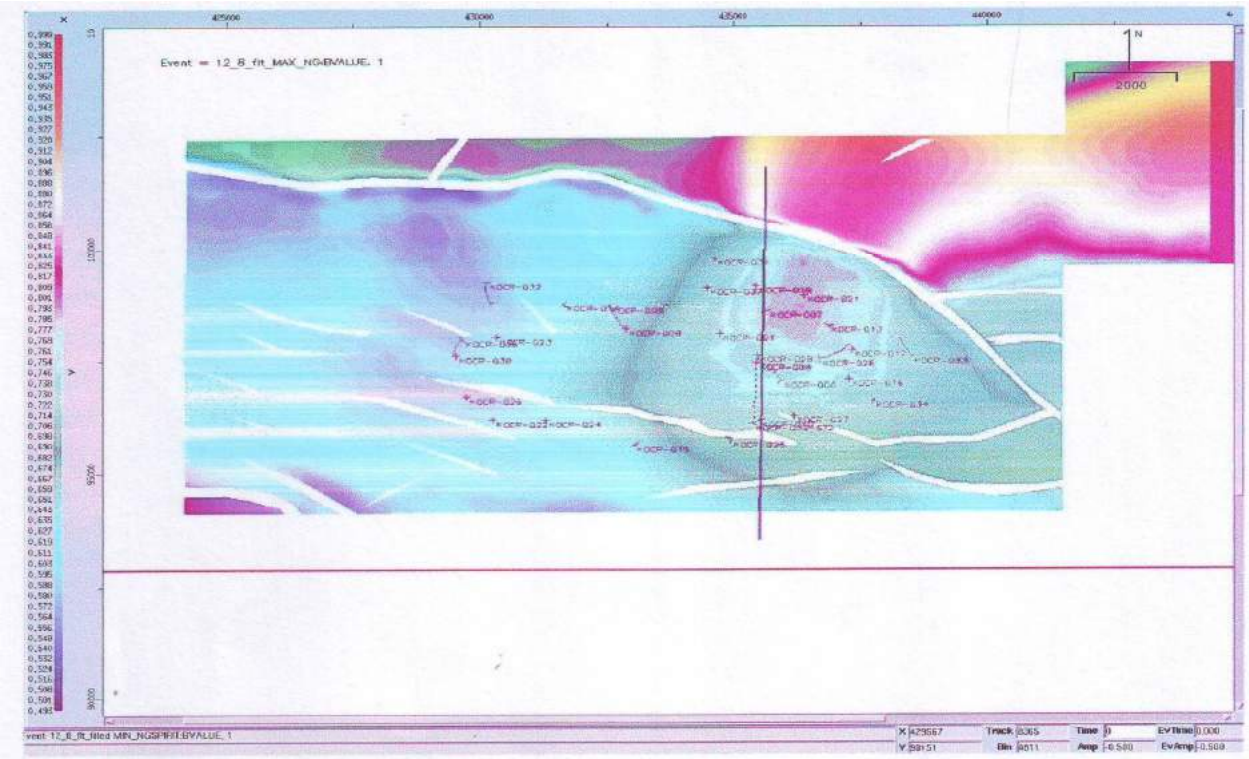

Fig. 12a. Predicted Maximum Net-to-Gross Map.

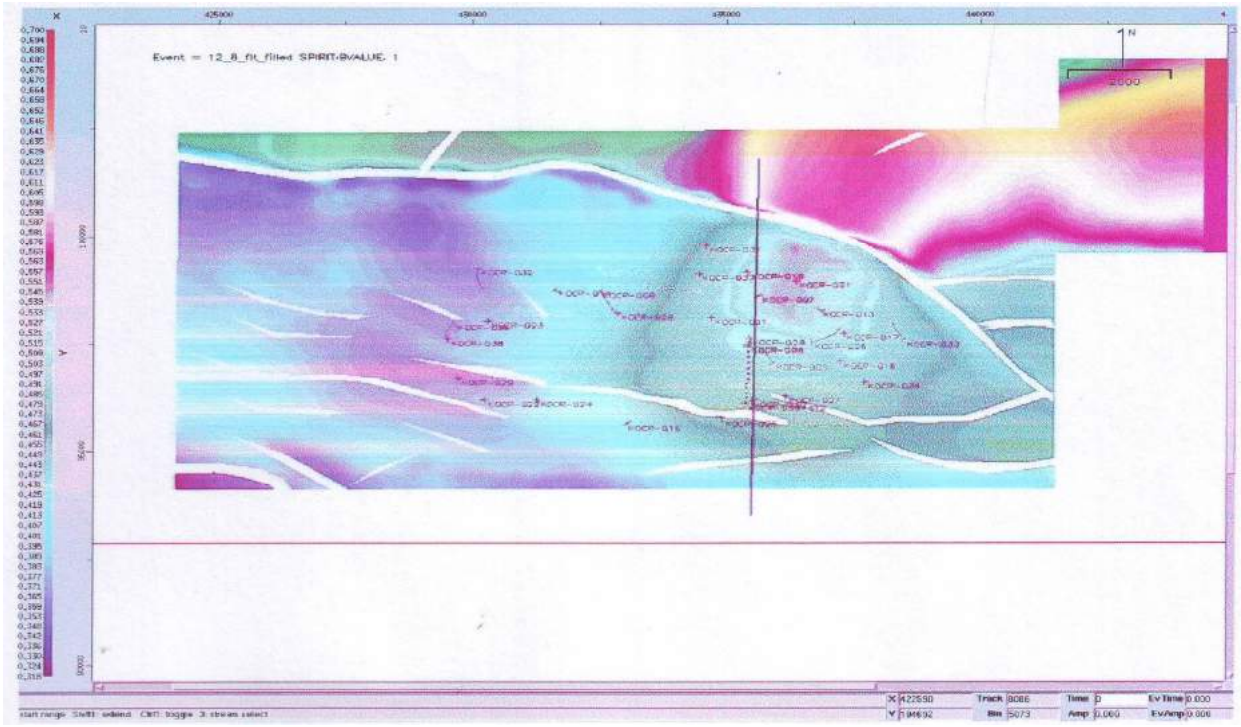

Fig. 12b. Predicted Most-likely Net-to-Gross Map.

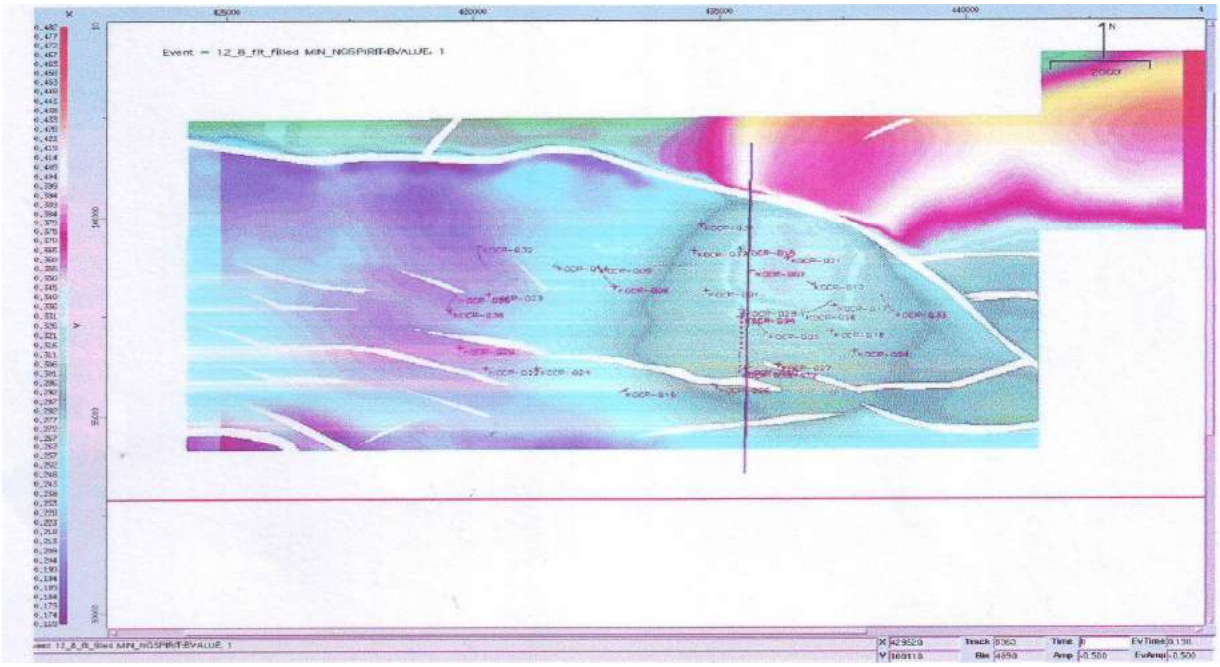

Fig. 12c. Predicted Minimum Net-to-Gross Map.

Net Sand Maps

Net-sand was obtained by multiplying the interval net-to-gross by the gross thickness of the interval. The gross thickness of the chosen interval (12.8MFS to 13.1SB) was extracted by subtracting the depth of the top horizon of the interval from the depth of the base of the interval. This gross thickness was calculated with the event calculator on *123Di* by using the depth maps of the interval 12.8MFS to 13.1SB as inputs and subtracting the shallower event from the deeper event. Figures13a, 13b, and 13c are the interval net-sand maps for the maximum, most-likely and minimum sand predictions.

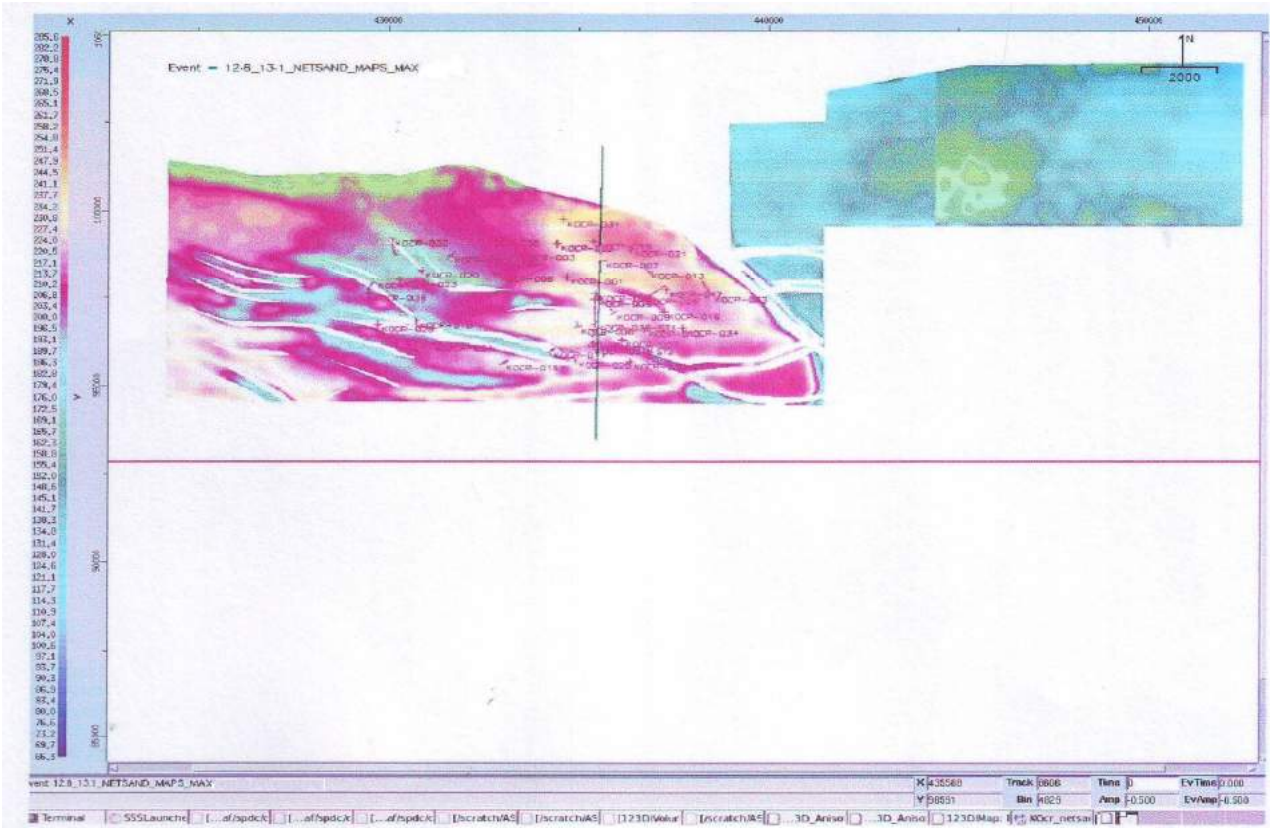

Fig. 13a. Maximum Interval (12.8MFS to 13.1SB) Net-Sand Map.

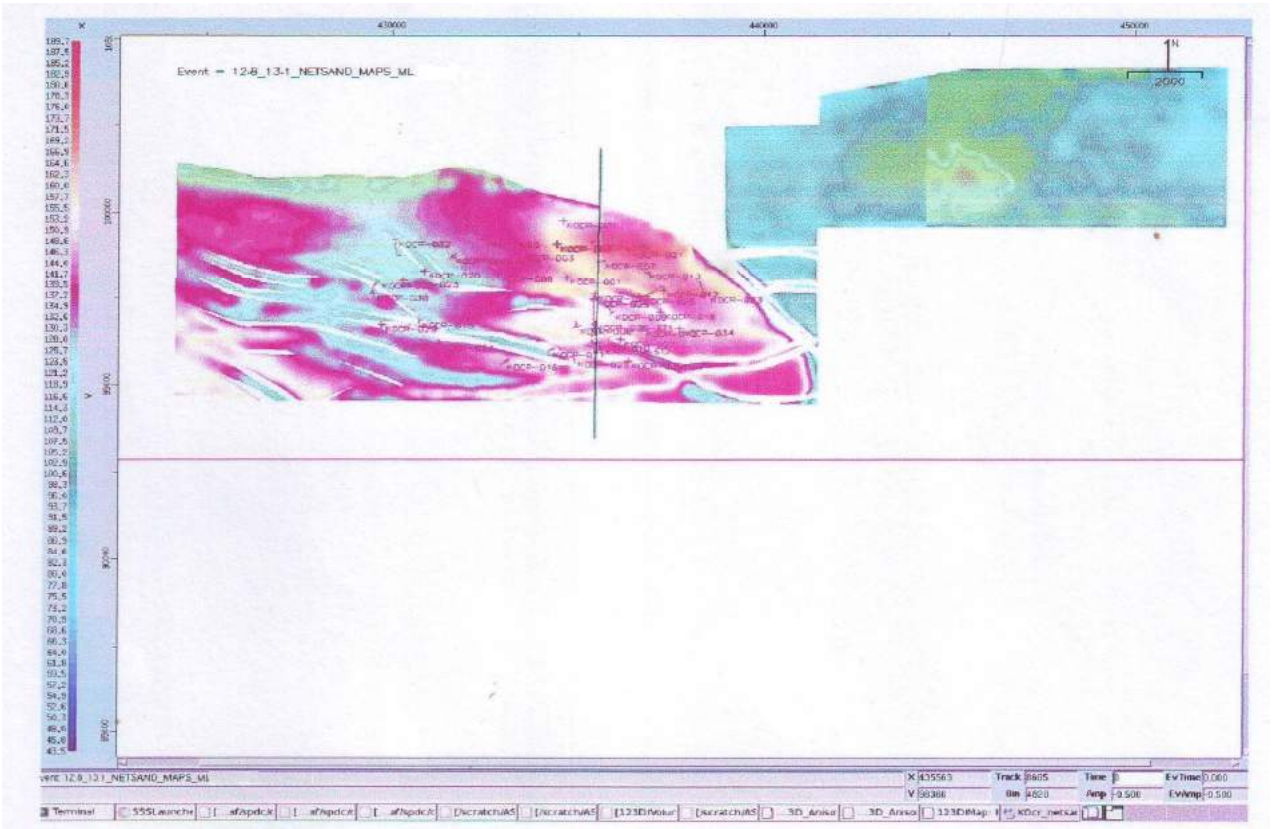

Fig. 13b. Most-likely Interval (12.8MFS to 13.1SB) Net-Sand Map.

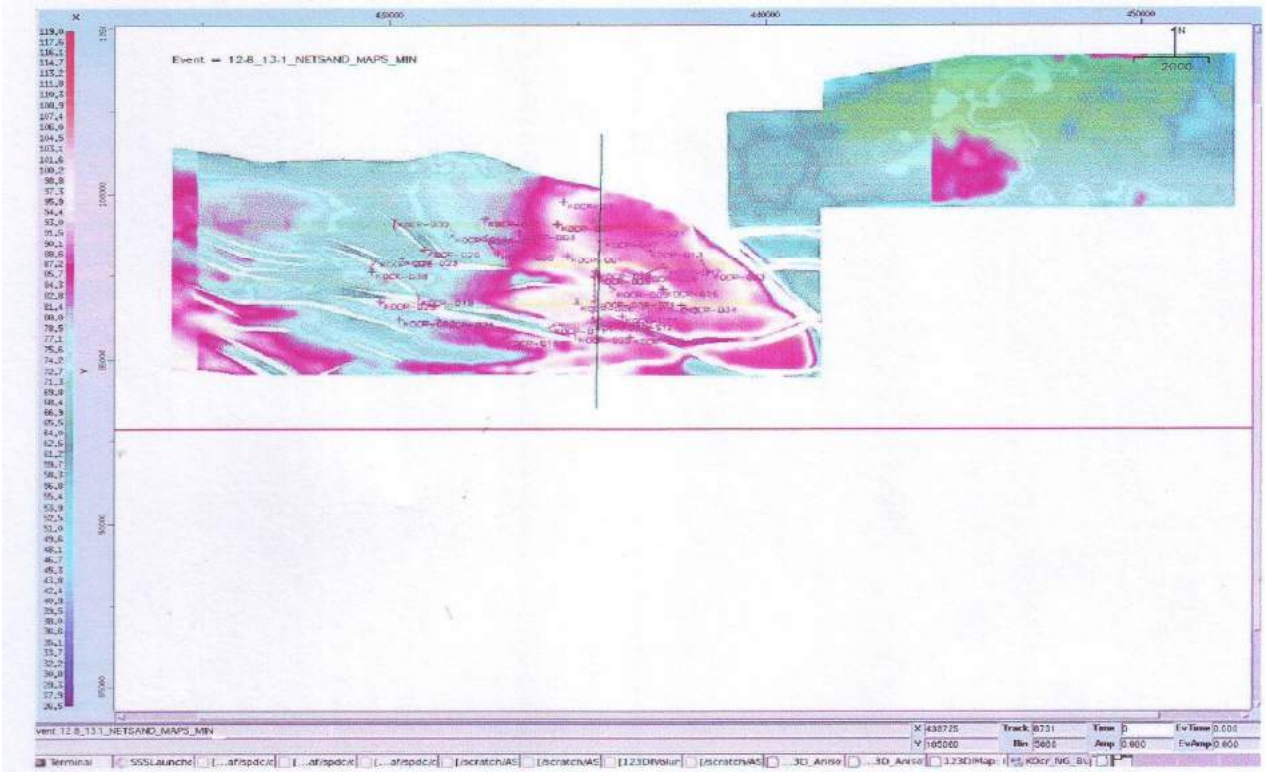

Fig. 13c. Minimum Interval (12.8MFS to 13.1SB) Net-Sand Map.

CONCLUSION AND RECOMMENDATION

The investigation reveals a consistent relation of eta, η increasing with increasing volume of shale, V_{sh}. The main source of anisotropy is believed to be thick interval shale formation. The study also reveals that seismic eta cube can be used to effectively predict interval net- sand that can have a positive impact on hydrocarbon exploration. More hydrocarbon volume can be derived from deep-seated structures which can be effectively mapped using an anisotropy-corrected seismic data. Eta band thickness should be made as close as possible to the thickness of the geologic intervals. It should be constrained to follow geologic events laterally rather than running flat. A seismic quality eta should be produced by Seismic Processors in order to filter non-hockey sticks from the eta cube. Further research should be conducted by integrating spectral decomposition with seismic anisotropy in the prediction of net-sand thickness.

ACKNOWLEDGEMENT

The authors express their gratitude to Shell Petroleum Development Company Nigeria Limited (SPDC) for access to the data and software used for this study. The staff of the Subsurface Services Department of SPDC are commended for their support. The Department of Petroleum Resources are also appreciated for data release approval.

REFERENCES

Alkhalifah, T. and Rampton, D. 2001. Seismic Anisotropy in Trinidad: A New Tool for Lithology Prediction. The Leading Edge. 20:420-424.

Brown, AR., Wright, RM., Burkart, KD. and Abriel, WL. 1984. Interactive Seismic Mapping of Net Producible Gas Sand in the Gulf of Mexico. Geophysics. 49:686-714.

Burge, DW. and Neff, DB. 1998. Well Based Seismic Lithology Inversion for Porosity and Pay-thickness Mapping. The Leading Edge. 17:166-171.

Chunduru, R. and Nordstrom, P. 2008. Seismic Inversion and Net Sand Estimation in Deep Water Turbidite Sands, Bonga Fields, Offshore Nigeria. 7th International Conference & Exposition on Petroleum Geophysics, Hyderabad. pp448.

Connolly, P., Schurter, G., Davenport, M. and Smith, S. 2002. Estimating Net Pay for Deep-Water Turbidite Channels Offshore Angola. 64th EAGE Conference & Exhibition, Extended Abstracts. G-28.

Connolly, P. 2005. Net Pay Estimation from Seismic Attributes. 67th EAGE Conference & Exhibition, Extended Abstracts. F016.

Johnston, JJ. and Christensen, NI. 1995. Seismic Anisotropy of Shales. Journal of Geophysical Research. 100, No. B4:5991-6003.

Kishore, M., Sharma, S., Kumar, B. and Srivastava, A. 2006. An Approach to Net Thickness Prediction using Spectral Decomposition. Geohorizons. pp58-61.

Li, Y. 2004. Anisotropic Parameter Prediction in Clastic Rocks. CSEG National Convention. pp1-5.

Oboh, FE. 1993. Depositional history of the E2.0 Reservoir in the Kolo Creek Field, Niger Delta. Journal of Petroleum Geology. 16:197-212.

Oboh, FE. 1995. Sedimentological and Palynological Characteristics of the E2.0 Reservoir (Miocene) in the Kolo Creek Field, Niger Delta. In: Geology of Deltas. Eds. Oti, M. and Postma, G. Rotterdam, Netherlands. pp315.

Okorie, IPC., Ebeniro, JO. and Ehirim, CN. 2016. Anisotropy and Empirical Relations for the Estimation of Anisotropy Parameters in Niger Delta Depobelts. International Journal of Geosciences. 7:345-352.

Ouadfeul, S. 2015. Contribution of the Seismic Anisotropy in the Understanding of Tight Sand Reservoir with an Example from Algeria Sahara. SEG New Orleans Annual Meeting. 331-335.

Simm, R. 2009. Simple Net Pay Estimation from Seismic: A Modelling Study. First Break. 27:45-53.

Schlumberger. 1996. Log Interpretation Charts. Schlumberger Well Services, Houston. 2-34.

Short, KC. and Stauble, AJ. 1967. Outline of Geology of Niger Delta. American Association of Petroleum Geologists Bulletin. 51:761-799.

Thomsen, L. 1986. Weak Elastic Anisotropy. Geophysics. 51:1954-1966.

Received: August 19, 2018; Accepted: Dec 17, 2019